Development 138, 667-676 (2011) doi:10.1242/dev.052803

Stringent requirement of a proper level of canonical WNT signalling activity for head formation in mouse embryo

Nicolas Fossat[1,2], Vanessa Jones[1], Poh-Lynn Khoo[1], Debora Bogani[3], Andrea Hardy[3], Kirsten Steiner[1], Mahua Mukhopadhyay[4], Heiner Westphal[4], Patrick M. Nolan[3], Ruth Arkell[3,5] and Patrick P. L. Tam[1,2,*]

SUMMARY

In mouse embryos, loss of Dickkopf-1 (DKK1) activity is associated with an ectopic activation of WNT signalling responses in the precursors of the craniofacial structures and leads to a complete truncation of the head at early organogenesis. Here, we show that ENU-induced mutations of genes coding for two WNT canonical pathway factors, the co-receptor LRP6 and the transcriptional co-activator β-catenin, also elicit an ectopic signalling response and result in loss of the rostral tissues of the forebrain. Compound mutant embryos harbouring combinations of mutant alleles of *Lrp6*, *Ctnnb1* and *Dkk1* recapitulate the partial to complete head truncation phenotype of individual homozygous mutants. The demonstration of a synergistic interaction of *Dkk1*, *Lrp6* and *Ctnnb1* provides compelling evidence supporting the concepts that (1) stringent regulation of the level of canonical WNT signalling is necessary for head formation, (2) activity of the canonical pathway is sufficient to account for the phenotypic effects of mutations in three different components of the signal cascade and (3) rostral parts of the brain and the head are differentially more sensitive to canonical WNT signalling and their development is contingent on negative modulation of WNT signalling activity.

KEY WORDS: Dkk1, Lrp6, β-Catenin, ENU mutant, WNT signalling, Head formation, Mouse, Gene dosage

INTRODUCTION

Formation of the head of the mouse embryo is accomplished by the coordinated regulation of specification, differentiation and movement of the progenitor cells, culminating in an orchestration of orderly growth and patterning of the brain and the facial primordia. These processes are driven by the morphogenetic activity elicited by inductive interactions between the primordial tissues of the head mediated by intercellular signalling. Analysis of gene expression patterns reveals that a multitude of genes encoding transcription factors and signalling molecules, among them inhibitors and components of the WNT signalling pathway, are activated in these tissues during head formation (Robb and Tam, 2004).

WNT (wingless and int) factors signal to the target cells by one of three transduction mechanisms: canonical WNT-β-catenin (for tissue patterning), WNT-planar cell polarity (WNT-PCP; for controlling cell shape and tissue remodelling) and WNT-calcium pathways [for calcium signalling and cell adhesion (Logan and Nusse, 2004)]. Signalling via the WNT-β-catenin pathway involves a cascade of molecular activity from binding of the WNT ligand to the cell surface receptor complex of frizzled (FZD) and lipoprotein receptor-related proteins (LRP5 and LRP6) and transduction of the signalling activity to the subsequent activation of responsive genes mediated by the transcriptional co-activator β-catenin (Fig. 1A). WNT signalling activity is negatively regulated by secreted proteins such as secreted frizzled-related proteins (SFRP) and DKK1. DKK1 dampens signalling activity by disengaging LRP6 from the receptor complex thereby blocking the WNT ligand-receptor interaction (Brott and Sokol, 2002; MacDonald et al., 2009).

Fate-mapping studies of mouse embryos at gastrulation and early organogenesis reveal that progenitors of the prospective telencephalon and diencephalon are always found in the region of the embryo with no or weaker WNT-reporter activity (Fig. 1B), suggesting that negative modulation of signalling activity is a prerequisite for normal development of the head. In the mouse, embryos lacking *Dkk1* activity display ectopic and elevated WNT signalling activity in precursor tissues of the embryonic head and fail to form brain and head structures (Lewis et al., 2008; Mukhopadhyay et al., 2001), whereas reduced *Dkk1* activity in the hypomorphic *Dkk1-doubleridge* mutant is associated with head malformation (MacDonald et al., 2004). Analysis of the phenotype of compound mutant embryos has revealed that the severity of head truncation defects caused by loss of *Dkk1* function might be enhanced by reducing the gene dosage of *Gsc* (Lewis et al., 2007), which acts to repress the transcription of WNT ligand genes (Yao and Kessler, 2001). By contrast, reducing the level of *Wnt3* activity is sufficient to allow normal head morphogenesis in some embryos that completely lack *Dkk1* activity (Lewis et al., 2008). A precedent study has also shown that the loss of *Dkk1* antagonist function might be compensated for by reduction of the function of the LRP6 co-receptor (MacDonald et al., 2004).

To assess further the impact of canonical WNT signalling activity in head development, we have conducted a genetic study of the interaction of DKK1 activity with two components of the signalling cascade: the LRP6 co-receptor (encoded by *Lrp6*) that

[1]Embryology Unit, Children's Medical Research Institute, University of Sydney, 214 Hawkesbury Road, Westmead, Sydney, NSW 2145, Australia. [2]Sydney Medical School, University of Sydney, Westmead, NSW 2145, Australia. [3]MRC Mammalian Genetics Unit, Harwell, OX11 0RD, Oxfordshire, UK. [4]Laboratory of Mammalian Genes and Development, Eunice Kennedy Shriver Institute of Child Health and Human Development, National Institutes of Health, Bethesda, MD 20892, USA. [5]ARC Special Research Centre for the Molecular Genetics of Development and Molecular Genetics and Evolution Group, Research School of Biological Sciences, The Australian National University, Canberra, ACT 2601, Australia.

*Author for correspondence (ptam@cmri.org.au)

Accepted 1 December 2010

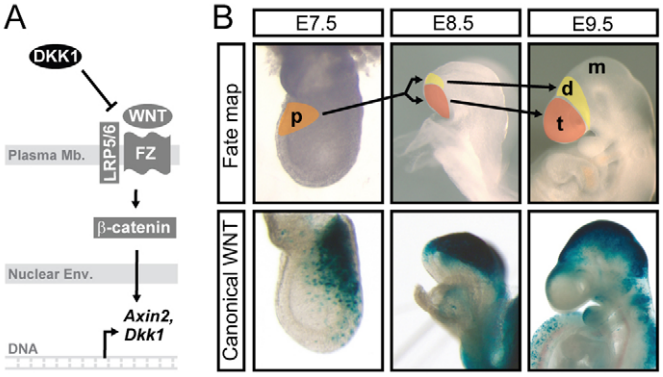

Fig. 1. Canonical WNT signalling activity in head tissue progenitors. (**A**) Schematic depicting the canonical WNT signalling cascade showing the ligand (WNT), co-receptor (LRP5, LRP6), receptor (frizzled; FZ), antagonist (DKK1), transcription co-activator (β-catenin) and target genes (*Axin2*, *Dkk1*). Env, envelope; Mb, membrane. (**B**) Localisation of the progenitors of prosencephalon (p) in the ectoderm of an E7.5 embryo and those of the prospective telencephalon (t), diencephalon (d) and mesencephalon (m) in E8.5 and E9.5 embryos (fate-maps; upper panels), correlated with the expression domain of the BATGal reporter, which reveals the response of tissues to canonical WNT signalling activity (lower panels). Data for fate-maps are based on Tam, Rubenstein et al. and Inoue et al. (Tam, 1989; Rubenstein et al., 1998; Inoue et al., 2000).

forms a complex with the frizzled receptor and the WNT ligand; and β-catenin (encoded by *Ctnnb1*), which is the co-activator acting with LEF and TCF transcription factors to regulate the transcription of WNT target genes (Fig. 1A). To study the genetic interaction between *Dkk1*, *Lrp6* and *Ctnnb1*, we utilised two mutants that were identified in screens of N-ethyl-N-nitrosourea (ENU)-mutagenised mice: gwazi (Bogani et al., 2004) and batface (Nolan et al., 2000). These two mutants harbour a point mutation in *Lrp6* and *Ctnnb1*, respectively, and they are associated with a gain of canonical WNT signalling activity and head truncation defects. Our analysis of compound mutants for *Dkk1*, *Lrp6* and *Ctnnb1* showed that repression of canonical WNT signalling by DKK1, mediated by interaction with the co-receptor LRP6 and the downstream transcriptional co-activator β-catenin, is essential for embryonic head formation. We also found that development of the rostral parts of the brain is particularly sensitive to canonical WNT signalling, underpinning the necessity of a stringent regulation of the domain and level of the WNT signalling response for craniofacial morphogenesis.

MATERIALS AND METHODS

Characterisation and genotyping strategy of the gwazi mutant mice

The *gwazi (Gw)* mutant was identified in an ENU mutagenesis screen for semi-dominant mouse mutants (Bogani et al., 2004) by the observation that heterozygous carriers of the mutation have a crooked tail (see Fig. S1A in the supplementary material). Genetic mapping localised the mutation to the mid portion of Mmu6. The genomic DNA of the non-recombinant region was scanned for nucleotide changes by sequence analysis of PCR amplified products of the coding region of the *Lrp6* gene. Of the 23 exons analysed, one showed a single base difference between the affected individuals and the pre-ENU treated parental (BALB/c) strains (Fig. 2A). A further 30 affected individuals were sequenced and all were found to harbour this nucleotide change. The variant product spanned exon 7 and was caused by a mis-sense mutation at nucleotide 1862 (accession #BC060704; see Fig. S1B in the supplementary material) resulting in D549G change (Fig. 2B) of a conserved region of the LRP proteins (see Fig. S1B in the supplementary material). Five other strains of mice (*Mus castaneus*, *Mus spretus*, C57BL/6J, 129Sv and 101/H) were analysed and none was found to contain the variant allele, suggesting that it is not a naturally occurring polymorphism. In the colony, which was maintained as heterozygotes on a C3H/HeH background, co-segregation of the mutation and phenotype was observed in over 200 meioses. These mice are heretofore referred to as *Lrp6-Gw* mice.

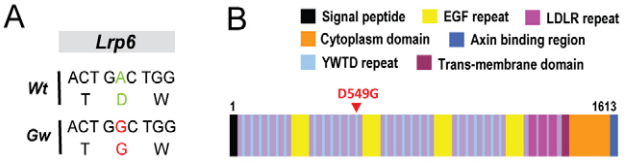

Fig. 2. *Lrp6-Gw* mutation. (**A**) An A to G change in the *Lrp6*^{Gw} allele leads to the D549G mutation of the LRP6 protein. Wt, wild type. (**B**) Localisation of the mutation in the last YWTD repeat of the second propeller domain of the LRP6 protein. Functional domains of the protein are colour-coded.

For genotyping, two independent PCRs were performed from the same DNA sample extracted from tail or yolk sac. Primers NF19.10 (5′-ACTATGTTTACTGGACTGA-3′) and NF21.1 (5′-GATCTAACCTA-ACAGATCACA-3′) amplified a fragment of 293 bp from the *Lrp6*$^{+}$ allele only. Conditions used were: 94°C for 30 seconds, 55°C for 60 seconds, 72°C for 45 seconds for 35 cycles. Primers NF19.1 (5′-ACTATGTTT-ACTGGACTGG-3′) and NF21.1 (5′-GATCTAACCTAACAGATCACA-3′) amplified a fragment of the same size from the *Lrp6*^{Gw} allele only (see Fig. S1C in the supplementary material). Conditions used were: 94°C for 30 seconds, 58°C for 60 seconds, 72°C for 45 seconds for 35 cycles.

Characterisation and genotyping strategy of the batface mutant mice

The *batface (Bfc)* mutant was isolated in a genetic screen for dominant mutations and the heterozygous mutants were identified by craniofacial dysmorphology (see Fig. S2A in the supplementary material) and aberrant neurological behaviour (Nolan et al., 2000). Genetic mapping localised the mutation to the distal region of Mmu9 and sequencing of genes in the non-recombinant interval identified a C to A transversion in the *Ctnnb1* gene resulting in a T653K change in the β-catenin protein (Fig. 3A,B) (P.M.N., unpublished). These mice are heretofore referred to as *Ctnnb1-Bfc* mice, which were maintained as heterozygotes separately on a C57/BL6 and BALB/c background.

For genotyping, two independent PCRs were performed from the same DNA sample extracted from tail or yolk sac. Primers NF19.3 (5′-AAAGAGTAGCTGCAGGGGT-3′) and NF18.1 (5′-GGACAGCAG-CTGCGTATG-3′) amplified a fragment of 235 bp from the *Ctnnb1*$^{+}$ allele only. Primers NF19.3 (5′-AAAGAGTAGCTGCAGGGGT-3′) and NF19.2 (5′-AGGACAGCAGCTGCGTATT-3′) amplified a fragment of 236 bp from the *Ctnnb1*^{Bfc} allele only (see Fig. S2C in the supplementary material). Conditions were similar for the two PCRs: 94°C for 30 seconds, 60°C for 30 seconds, 72°C for 45 seconds for 35 cycles.

RNA isolation and RT-qPCR

To assess the expression of *Axin2*, embryonic day (E)8.5 stage-matched (two to six somites) embryos harvested from pregnant mice of *Ctnnb1*$^{Bfc/+}$ × *Ctnnb1*$^{Bfc/+}$ crosses were dissected in PBS, staged for developmental status and frozen whole. The embryos were genotyped using the yolk sac material. To determine the level of expression of *Axin2*, *Dkk1* and *Sfrp1*, E9.5 stage-matched (20-25 somites) embryos harvested from pregnant mice of *Ctnnb1*$^{Bfc/+}$ × *Dkk1*$^{+/-}$;*Lrp6*$^{Gw/Gw}$ crosses were dissected in PBS, staged and categorised. Head and body parts were separated by cutting transversely at the level immediately posterior to the otic vesicle (Fig. 4A) and were frozen separately. The embryos were genotyped using the yolk sac material. Extraction of total RNA was carried out independently for

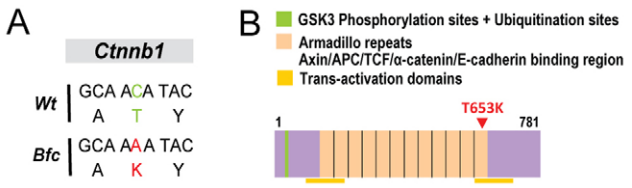

Fig. 3. *Ctnnb1-Bfc* mutation. (**A**) A C to A change in the *Ctnnb1*^{Bfc} allele leads to the T653K mutation of the β-catenin protein. Wt, wild type. (**B**) Localisation of the mutation in the last armadillo repeat of the β-catenin protein. Functional domains of the protein are colour-coded.

each sample (whole E8.5 embryo; head or body part of E9.5 embryo) using the RNeasy Micro Kit (Qiagen). First strand cDNA was synthesised using 100 ng (whole E8.5 embryo, head part of E9.5 embryo) or 300 ng (body part of E9.5 embryo) of mRNA and the SuperScript III First Strand System (Invitrogen). Quantitative PCR was performed in triplicate from 1:3 dilution of cDNA of each sample using the Rotorgene 6000 thermal cycler (Corbett Research), SYBR Green I (Molecular Probes) and Platinum Taq DNA Polymerase (Invitrogen). Primers 5′-ACCTCAAGTGCAAAC-TCTCA-3′ and 5′-GTGATAAGGATTGACTGGGT-3′ amplify a fragment of 140 bp from *Axin2* cDNA. Primers 5′-TTGGTAATGACCACAA-CGCCGC-3′ and 5′-GGAATATCTCCAGCCCGTGGGA-3′ amplify a fragment of 237 bp from *Dkk1* cDNA. Primers 5′-CCATGC-GACAACGAGTTGA-3′ and 5′-GTTCTTCAGGAACAGCACAA-3′ amplify a fragment of 195 bp from *Sfrp1* cDNA. Primers 5′-AGC-ACCCTGTGCTGCTCA-3′ and 5′-GTACGACCAGAGGCATACA-3′ amplify a fragment of 145 bp from β-*actin* cDNA. Conditions were similar for all the PCRs: 94°C for 30 seconds, 62°C for 30 seconds, 72°C for 20 seconds for 40 cycles. Fluorescence was read at the end of each elongation step. A melting curve was plotted at the end of the run to check that only the fragment of interest had been amplified.

Genotyping and breeding strategy of Dkk1, Wnt3 and BATGal mice and the generation of compound mutants

The genotyping of *Dkk1* mutant mice (Mukhopadhyay et al., 2001), *Wnt3* mutant mice (Liu et al., 1999) and BATGal mice (Maretto et al., 2003) followed the established protocol. Genotyping by PCR was performed on DNA extraction from tail tissues of newborn mice or the yolk sac of embryos. The breeding strategy for the production of compound mutant mice as well as the number of adults and embryos obtained for each genotype are given in Table 1 and Tables S1-S6 in the supplementary material.

X-Gal staining

Lrp6$^{Gw/+}$;BATGal:BATGal × *Lrp6*$^{Gw/+}$ and *Ctnnb1*$^{Bfc/+}$;BATGal:BATGal × *Ctnnb1*$^{Bfc/+}$ intercrosses were performed to produce embryos that were uniformly BATGal heterozygous irrespective of other aspects of the genotype. X-Gal staining was performed as described by Lewis et al. (Lewis et al., 2008). Specimens of different genotypes were processed in the same run to ensure that the staining results could be compared.

Phenotypic analysis

The mutant embryos were examined for head morphology in comparison with wild-type embryos of the same age. The degree of head truncation was determined by morphometric measurement of the head size of E9.5 embryos (see legend for Fig. 4A). Based on the degree of head truncation, embryos of various genotypes were assigned to one of the five phenotype categories: [I] normal head size (0%) and morphology comparable to the wild-type embryo, [II] ≤25 % reduction of the forebrain, [III] 26-75% reduction of the forebrain, [IV] >75% reduction but with recognisable remnant of the forebrain and [V] phenocopy of the complete head truncation (100%) of *Dkk1*-null embryo (Fig. 4B).

In situ hybridisations with *Six3*, *Fgf8*, *Emx2*, *Hesx1*, *Tcf4*, *En2*, *Cer1*, *Foxa2*, *Lhx1* and *Shh* riboprobes were performed on between two and eight specimens of each specified genotype as described by Simeone et al. (Simeone et al., 1992), Fossat et al. (Fossat et al., 2007), Lewis et al. (Lewis et al., 2008) and Lavado et al. (Lavado et al., 2008).

RESULTS

Lrp6-Gw mutation causes a gain of WNT signalling function

Gwazi (Gw) mice were identified in an ENU-mutagenesis screen by their kinked tail, which is caused by the intercalation of a sesamoid bone between the caudal vertebrae (see Fig. S1A in the supplementary material) (Bogani et al., 2004). We identified the causative mutation in the seventh coding exon of the *Lrp6* gene, resulting in the substitution of a highly conserved aspartic acid with glycine (D549G) in the last YWTD repeat of the second propeller domain of the LRP6 protein (Fig. 2A,B). A bent tail was found in 67.5% of *Lrp6*$^{Gw/+}$ and 85.5% of *Lrp6*$^{Gw/Gw}$ mice (see Table S1A in the supplementary material). The frequency of tail kinks increased to 100% in *Dkk1*$^{+/–}$;*Lrp6*$^{Gw/+}$ mice, showing that the *Lrp6-Gw* mutant phenotype is enhanced with the elevation of WNT signalling activity caused by reduced DKK1. By contrast, the frequency of tail kinks dropped to 21.5% owing to the reduction of WNT signalling activity in *Wnt3*$^{+/–}$;*Lrp6*$^{Gw/+}$ mice (see Table S1B in the supplementary material). These results strongly suggest that the tail kink is associated with a gain of WNT function due to the *Lrp6-Gw* mutation, which is enhanced by the *Dkk1*-null mutation and suppressed by reduced *Wnt3* activity. Further support of the gain-of-function effect of the *Lrp6-Gw* mutation is the expanded expression domain of Lef-Tcf-promoter-*lacZ* reporter (BATGal) (Maretto et al., 2003). BATGal expression is normally regionalised to the posterior germ layers of the E7.5 embryo and is absent from

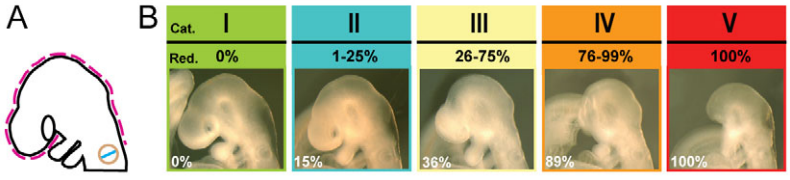

Fig. 4. Phenotype analysis of mutant embryos. (**A**) Morphometric analysis of head size of E9.5 embryos. The measurement is expressed as the ratio of the linear distance along the silhouette of the head from the border of the mandibular arch and maxillary prominence to the rostral margin of the otic vesicle (pink dashed line), and the diameter (blue line) of the otic vesicle (brown circle); the latter is relatively constant among embryos of the different genotypes (see also Lewis et al., 2007). The computed values of wild type and the most truncated (*Dkk1*-null-like) heads were normalized as 0% and 100% reduction of head size, respectively. (**B**) Phenotypic classification of the mutant embryo based on the morphology and degree of reduction of the head: Category (Cat.) I, normal; II-IV, partial truncation; V, most severe truncation. The range of the percentage of head size reduction (Red.) and the scores of the specimen (I, *Lrp6*$^{Gw/+}$; II and III, *Lrp6*$^{Gw/+}$;*Ctnnb1*$^{Bfc/+}$; IV and V, *Dkk1*$^{+/–}$;*Lrp6*$^{Gw/+}$;*Ctnnb1*$^{Bfc/+}$) for each category are shown.

Table 1. Frequency of head defects in WNT signalling mutants

Genotype of E9.0-10.0 embryos	Number of embryos with head defects/number analysed	Percentage of embryos with head defects
Wild type	1/73	1.5
Lrp6$^{Gw/+}$	8/124	6.5
Dkk1$^{+/-}$	2/23	8.5
Ctnnb1$^{Bfc/+}$	9/34	26.5*
Lrp6$^{Gw/Gw}$	8/27	29.5*
Dkk1$^{+/-}$;*Lrp6*$^{Gw/+}$	19/44	43*
Dkk1$^{+/-}$;*Lrp6*$^{Gw/Gw}$	11/14	78.5*
Lrp6$^{Gw/+}$;*Ctnnb1*$^{Bfc/+}$	37/43	86*
Dkk1$^{+/-}$;*Ctnnb1*$^{Bfc/+}$	23/25	92*
Ctnnb1$^{Bfc/Bfc}$	10/10	100*
Dkk1$^{+/-}$;*Ctnnb1*$^{Bfc/Bfc}$	3/3	100†
Dkk1$^{+/-}$;*Lrp6*$^{Gw/+}$;*Ctnnb1*$^{Bfc/+}$	22/22	100*

*Significantly different from wild type at $P<0.001$ by χ^2-test.
†Sample size too small for testing.

the progenitors of the prospective forebrain (Fig. 1B). In *Lrp6*$^{Gw/Gw}$ embryos at E7.5, BATGal expression expanded to the anterior germ layer tissues (8/14=57% embryos; Fig. 5A), reminiscent of previous observations in *Dkk1*$^{-/-}$ embryos (see Fig. S3A in the supplementary material) (Lewis et al., 2008). By E8.5-9.5, the BATGal expression domain extended further anteriorly (Fig. 5A; see Fig. S1D in the supplementary material). The *Lrp6*^{Gw} allele is therefore associated with a gain of WNT signalling function.

Lrp6$^{Gw/Gw}$ mutant embryos display head defects

Embryos lacking *Dkk1* activity displayed fully penetrant and complete truncations of the head (see Fig. S3B in the supplementary material) (Lewis et al., 2007; Lewis et al., 2008; Mukhopadhyay et al., 2001). To test if the gain of WNT function caused by the *Lrp6-Gw* mutation affects embryonic head formation similarly to that of loss of DKK1 function, we examined early organogenesis-stage embryos produced by crossing heterozygous *Lrp6*$^{Gw/+}$ mutant mice.

In the E10.0-11.0 litters of *Lrp6-Gw* mice, wild type, *Lrp6*$^{Gw/+}$ and *Lrp6*$^{Gw/Gw}$ embryos were present in the expected Mendelian ratio (Table S2 in the supplementary material). A reduced forebrain size (Class II and III) was found in 38.5% of E9.5 (Fig. 5B) and E10.5 *Lrp6*$^{Gw/Gw}$ embryos (see Fig. S1E in the supplementary material). The head morphology of the remaining 61.5% of *Lrp6*$^{Gw/Gw}$ embryos and the majority (94.5%) of the *Lrp6*$^{Gw/+}$ embryos was indistinguishable from that of wild-type littermates (Class I, Fig. 5B; see Fig. S1E and Table S2 in the supplementary material). The region affected corresponds to the zone of no to weak WNT activity in normal embryo (Fig. 1B), and where WNT signalling is expanded to in the *Lrp6*$^{Gw/Gw}$ mutants (Fig. 5A; see Fig. S1D in the supplementary material). To assess the impact of the gwazi mutation on the formation and relative size of the brain parts, we performed in situ hybridisation analysis of five marker genes that delineate rostral-ventral telencephalon and optic evagination (*Six3*), rostral telencephalon (anterior neural ridge; *Fgf8*), posterior-ventral telencephalon/ventral diencephalon (*Hesx1*), dorsal and lateral telencephalon (*Emx2*) and dorsal diencephalon (also expressed weakly in the ventral diencephalon, *Tcf4*) (Fig. 5C). Analysis of the expression of these region-specific markers, in comparison with that in the *Lrp6*$^{Gw/+}$ embryos, revealed the dorsal displacement of a reduced *Six3* and *Fgf8* expression domain, and a receding domain of *Emx2* expression in the *Lrp6*$^{Gw/Gw}$ embryos. By contrast, the *Hesx1* domain in the ventral diencephalon and the *Tcf4* domain in the dorsal diencephalon were unchanged. Collectively, these findings point to a reduction of the size of the rostral and dorsal telencephalon in *Lrp6*$^{Gw/Gw}$ embryos.

Lrp6-Gw mutation interacts genetically with Dkk1-null allele in head formation

The data so far have shown that the head phenotype of the *Lrp6*$^{Gw/Gw}$ embryos might be associated with a gain of WNT activity. Because DKK1 physically interacts with LRP6 to modulate the signalling activity of the receptor complex (Mao et al., 2001; Semenov et al., 2001), we tested whether there is an interaction between the *Lrp6*^{Gw} allele and the *Dkk1*$^{-}$ allele, which should enhance the head deficiency phenotype.

Three intercrosses of *Lrp6-Gw* and *Dkk1*-null mutant mice were performed from which embryos of six genotypes were produced (see Table S3A in the supplementary material). When examined at the early organogenesis-stage, *Dkk1*$^{+/-}$ embryos were morphologically similar to the wild-type embryos and 9.5% of the *Lrp6*$^{Gw/+}$ embryos displayed abnormal forebrain (Class II). The frequency of head abnormality (Class II and III) increased to 39.5% in the *Dkk1*$^{+/-}$;*Lrp6*$^{Gw/+}$ embryos, which was comparable to the frequency of 33% observed for *Lrp6*$^{Gw/Gw}$ embryos (Fig. 5D; see Table S3A in the supplementary material). Marker analysis revealed very similar changes in the *Six3*, *Fgf8*, *Emx2*, *Hesx1* and *Tcf4* expression domain in the *Dkk1*$^{+/-}$;*Lrp6*$^{Gw/+}$ and *Lrp6*$^{Gw/Gw}$ embryos (Fig. 5C,D) suggesting that, like the *Lrp6*$^{Gw/Gw}$ abnormal embryos, there is a reduction of the size of the telencephalon. An increase in the penetrance of the head phenotype (to 78.5%) was found in the *Dkk1*$^{+/-}$;*Lrp6*$^{Gw/Gw}$ embryos (see Table S3A in the supplementary material). These findings are consistent with the hypothesis that the *Lrp6*^{Gw} and *Dkk1*$^{-}$ alleles interact synergistically in a gene-dosage-dependent manner to influence the head size, reinforcing the idea that DKK1 interacts functionally with LRP6 in regulating WNT signalling activity for head morphogenesis.

Ctnnb1-Bfc mutation causes a gain of WNT signalling function and head defects

The demonstration of a positive genetic interaction of *Lrp6* and *Dkk1* implies the involvement of the canonical signalling pathway in regulating head morphogenesis and that a gain of WNT function underpins the abnormal phenotype. However, it is necessary to test more specifically whether the phenotypic effect is mediated by the intracellular transcriptional co-activator, β-catenin, which is downstream of LRP6 and DKK1 in the canonical signalling cascade.

Batface (Bfc) mice were identified in an ENU-mutagenesis screen by their bat-like squashed face (see Fig. S2A in the supplementary material) (Nolan et al., 2000). We mapped the causative mutation to the thirteenth coding exon of the *Ctnnb1*

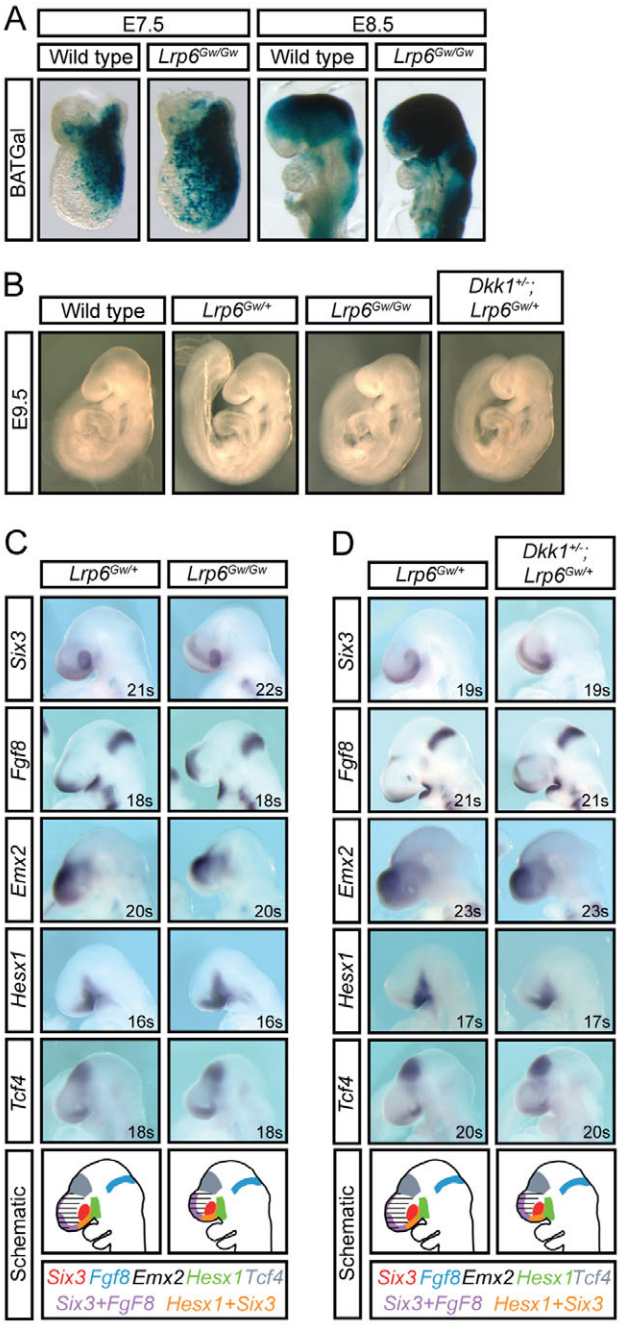

Fig. 5. Phenotype of *Lrp6-Gw* mutant embryos. (**A**) Expression of the *Tcf-Lef-lacZ* reporter (BATGal) in E7.5 (early bud stage) and E8.5 (early somites stage) wild-type and $Lrp6^{Gw/Gw}$ embryos. (**B**) Morphological appearance of wild-type, $Lrp6^{Gw/+}$, $Lrp6^{Gw/Gw}$ and $Dkk1^{+/-}$;$Lrp6^{Gw/+}$ E9.5 embryos. (**C**,**D**) *Six3*, *Fgf8*, *Emx2*, *Hesx1* and *Tcf4* expression in E9.0-9.5 $Lrp6^{Gw/Gw}$ embryos compared with $Lrp6^{Gw/+}$ embryos (C), and E9.0-9.5 $Dkk1^{+/-}$;$Lrp6^{Gw/+}$ embryos compared with $Lrp6^{Gw/+}$ embryos (D). Embryos were stage-matched by somite number (s). The in situ hybridisation data collated in the schematic diagrams highlight the difference in the expression pattern of the markers (colour-coded) in the head of $Lrp6^{Gw/+}$, $Lrp6^{Gw/Gw}$ and $Dkk1^{+/-}$;$Lrp6^{Gw/+}$ embryos.

gene, resulting in a T653K change in the last armadillo repeat of the β-catenin protein (Fig. 3A,B). In litters produced from intercrosses of heterozygous $Ctnnb1^{Bfc/+}$ mice, no viable homozygous offspring were found. In litters produced by crossing $Ctnnb1^{Bfc/+}$ and $Ctnnb1^{+/+}$ mice, heterozygous offspring were under-represented (27% on C57BL/6 background and 38.5% on BALB/c background, versus the expected 50%; see Table S4A in the supplementary material), suggesting that the viability of heterozygotes is compromised. On C57BL/6 and BALB/c background, all heterozygous $Ctnnb1^{Bfc/+}$ mice displayed a bat-like face with squashed snout. Furthermore, 23% $Ctnnb1^{Bfc/+}$ (C57BL/6) and 10.5% $Ctnnb1^{Bfc/+}$ (BALB/c) heterozygous mice also displayed ocular defects (Fig. S2A; see Table S4A in the supplementary material), including microphthalmia, anophthalmia and cataract-like clouding of the lens. There was a distortion of the genotype ratio of the offspring produced by crosses of $Dkk1^{+/-}$ and $Ctnnb1^{Bfc/+}$ mice, with a greatly reduced number of compound heterozygous $Dkk1^{+/-}$;$Ctnnb1^{Bfc/+}$ mice (5.5% versus the expected 25%; see Table S4B in the supplementary material). $Dkk1^{+/-}$;$Ctnnb1^{Bfc/+}$ mice also showed a higher incidence of ocular defects (71.5 %; see Table S4B in the supplementary material) than $Ctnnb1^{Bfc/+}$ mice of either the C57BL/6 or the BALB/c background. The enhanced impact on viability and ocular development of the $Ctnnb1^{Bfc/+}$ mice caused by genetically ablating one *Dkk1* allele thus suggests that the $Ctnnb1^{Bfc}$ allele is associated with an increase of WNT signalling activity. Analysis of BATGal expression in the $Ctnnb1^{Bfc/Bfc}$ mutant embryos revealed an expansion of the expression domain to anterior tissues at E7.5 (7/8 embryos), E8.5 and E9.5 (all embryos) (Fig. 6A; see Fig. S2D in the supplementary material), similar to that found in the $Lrp6^{Gw/Gw}$ and $Dkk1^{-/-}$ embryos. In addition, RT-qPCR analysis showed upregulation of a WNT downstream target, *Axin2*, in E8.5 $Ctnnb1^{Bfc/+}$ and $Ctnnb1^{Bfc/Bfc}$ embryos (see Fig. S2E in the supplementary material). $Ctnnb1^{Bfc}$ allele is therefore likely to be a gain of WNT function mutation.

As the *Ctnnb1-Bfc* mutation might cause a gain of WNT function, we examined whether it affects embryonic head formation similarly to the $Lrp6^{Gw/Gw}$ and $Dkk1^{-/-}$ mutants. Of the heterozygous $Ctnnb1^{Bfc/+}$ embryos, 37.5% at E8.0-9.0 and 89.5% at E9.0-11.0 displayed head defects characterised by a reduced forebrain (Class II; Fig. 6B; see Fig. S2F in the supplementary material), which is reminiscent of the $Lrp6^{Gw/Gw}$ phenotype. $Ctnnb1^{Bfc/Bfc}$ embryos recovered in E7.0-11.0 litters (19.5% of all embryos) on the C57BL/6 background (see Table S5 in the supplementary material) all displayed the strong phenotype (Class IV) of forebrain truncation (E9.5, Fig. 6B; E10.5, see Fig. S2F and Table S5 in the supplementary material). Analysis of *Six3* and *Fgf8* expression revealed a marked reduction of these telencephalon markers in the $Ctnnb1^{Bfc/+}$ embryos and very weak to no expression in the $Ctnnb1^{Bfc/Bfc}$ embryos (Fig. 6C). *Hesx1* and *Tcf4* expression was not affected in $Ctnnb1^{Bfc/+}$ embryos despite an overall reduced size of the forebrain. By contrast, *Hesx1* expression was almost absent and *Tcf4* expression domain was reduced and displaced to a more rostral region in the truncated brain of $Ctnnb1^{Bfc/Bfc}$ embryos (Fig. 6C). These findings suggest that the telencephalon is reduced in $Ctnnb1^{Bfc/+}$ embryos and is absent in $Ctnnb1^{Bfc/Bfc}$ embryos, which also have a smaller diencephalon.

To study the interaction between $Ctnnb1^{Bfc}$ and $Dkk1^{-}$ alleles, two intercrosses were performed to produce embryos of six genotypes (see Table S3B in the supplementary material). On the BALB/c background, 23% $Ctnnb1^{Bfc/+}$ embryos displayed deficiency of head tissues (Class II). This frequency was increased to 95% in $Dkk1^{+/-}$;$Ctnnb1^{Bfc/+}$ embryos (Fig. 6B; see Table S3B in the supplementary material), whereas 9% of $Dkk1^{+/-}$ embryos and

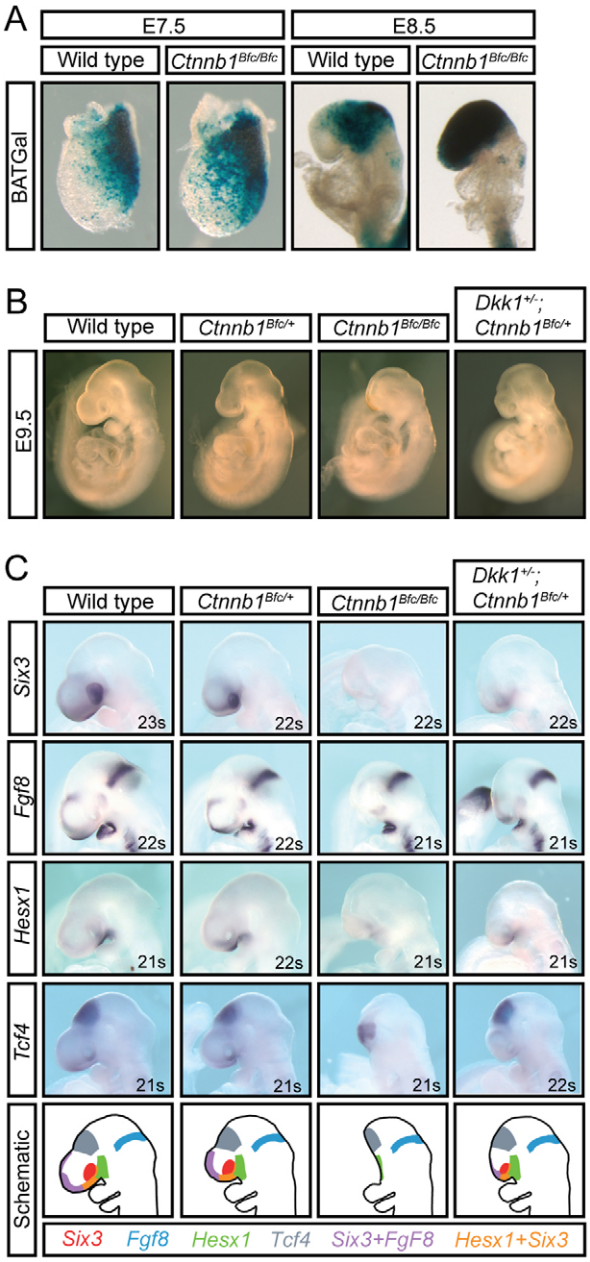

Fig. 6. Phenotype of *Ctnnb1-Bfc* mutant embryos. (**A**) Expression of the *Tcf-Lef-lacZ* reporter (BATGal) in E7.5 (early bud stage) and E8.5 (early somites stage) wild-type and $Ctnnb1^{Bfc/Bfc}$ mutant embryos. (**B**) Morphological appearance of wild-type, $Ctnnb1^{Bfc/+}$, $Ctnnb1^{Bfc/Bfc}$ and $Dkk1^{+/-}$;$Ctnnb1^{Bfc/+}$ E9.5 embryos. (**C**) *Six3*, *Fgf8*, *Hesx1* and *Tcf4* expression in E9.5 $Ctnnb1^{Bfc/+}$, $Ctnnb1^{Bfc/Bfc}$ and $Dkk1^{+/-}$;$Ctnnb1^{Bfc/+}$ embryos compared with wild-type embryos. Embryos were stage-matched by somite number (s). The gene expression data are collated in schematic diagrams to highlight the changes in the expression domain of the markers (colour-coded) in the head of $Ctnnb1^{Bfc/+}$, $Ctnnb1^{Bfc/Bfc}$ and $Dkk1^{+/-}$;$Ctnnb1^{Bfc/+}$ embryos compared with wild-type embryos.

100% of $Ctnnb1^{Bfc/Bfc}$ and $Dkk1^{+/-}$;$Ctnnb1^{Bfc/Bfc}$ embryos showed head reduction defects (see Table S3B in the supplementary material). E9.5 $Dkk1^{+/-}$;$Ctnnb1^{Bfc/+}$ embryos showed a reduced expression domain of *Six3*, *Fgf8* and *Hesx1* in the forebrain, which was intermediate in degrees between that of $Ctnnb1^{Bfc/+}$ and $Ctnnb1^{Bfc/Bfc}$ embryos (Fig. 6C). The enhanced manifestation of an abnormal head phenotype in $Dkk1^{+/-}$;$Ctnnb1^{Bfc/+}$ embryos provides compelling evidence for a positive genetic interaction of the $Ctnnb1^{Bfc}$ and $Dkk1^{-}$ alleles in head formation.

Gene dosage-dependent effects on the manifestation of mutant phenotypes

The functional connection between *Lrp6*, *Dkk1* and *Ctnnb1* in head morphogenesis was investigated by examining different combinations of the three alleles in embryos of eight genotypes obtained from four intercrosses (see Table S6 in the supplementary material). As expected from previous results showing an interaction between $Dkk1^{-}$ and $Lrp6^{Gw}$ alleles and between $Dkk1^{-}$ and $Ctnnb1^{Bfc}$ alleles, a genetic interaction between $Ctnnb1^{Bfc}$ and $Lrp6^{Gw}$ alleles was revealed by a severe head deficiency phenotype in 86% of the $Lpr6^{Gw/+}$;$Ctnnb1^{Bfc/+}$ double heterozygous mutants, compared with 5-15% of the single heterozygous ($Lrp6^{Gw/+}$ and $Ctnnb1^{Bfc/+}$) mutants. The double heterozygous $Lpr6^{Gw/+}$;$Ctnnb1^{Bfc/+}$ embryos phenocopied the deficiency of the compound $Dkk1^{+/-}$;$Lrp6^{Gw/Gw}$ and $Dkk1^{+/-}$;$Ctnnb1^{Bfc/+}$ embryos, and displayed similar changes in gene expression in the telencephalon (Fig. 7A,B and Fig. 6C). Furthermore, we observed that all of the triple compound $Dkk1^{+/-}$;$Lpr6^{Gw/+}$;$Ctnnb1^{Bfc/+}$ embryos developed head defects (see Table S6 in the supplementary material), with 23% of them showing a phenocopy of the complete truncation (Class V) of the $Dkk1^{-/-}$ embryos (Fig. 7A; see Fig. S3B in the supplementary material). Analysis of marker expression showed that these severely affected embryos completely lacked *Fgf8*- and *Tcf4*-expressing forebrain structures, and the *En2*-expressing tissues (the presumptive mesencephalon) were localised at the rostral-most position in the head (Fig. 7B). In the triple-mutant brain, *Fgf8* expression at the presumptive mesencephalon/metencephalon boundary appeared to be unaffected (Fig. 7B). These results point to a positive genetic interaction of the $Dkk1^{-}$, $Lrp6^{Gw}$ and $Ctnnb1^{Bfc}$ alleles in head formation.

Head truncation is associated with elevated canonical WNT signalling activity

Collectively, the outcomes of the genetic interaction study infer that these three components of the canonical WNT signalling pathway are functionally integrated into the molecular mechanism of head morphogenesis in the mouse embryo. These data also suggest that proper regulation of the canonical WNT signalling activity is essential for the formation of the rostral parts of the brain and the head. The collated data (Table 1) showed that the impact of mutation, as revealed by enhancement of the mutant phenotype, is influenced by the gene dosage, with the severity of defects increasing in the order of *Lrp6-Gw*<*Ctnnb1-Bfc*<*Dkk1*-null alleles.

In view of the observation that head morphogenesis is influenced by the signalling activity of embryonic tissues such as the anterior visceral endoderm and the organiser-derived anterior mesendoderm and anterior notochord, marker analysis was performed to examine whether these tissues are formed properly in the mutant embryos. Three types of mutant embryos with different penetrance of head phenotype (Table 1) were examined: $Lrp6^{Gw/+}$ (single mutant, 6.3%), $Lrp6^{Gw/+}$;$Ctnnb1^{Bfc/+}$ (double heterozygotes, 86%) and $Dkk1^{+/-}$;$Lrp6^{Gw/+}$;$Ctnnb1^{Bfc/+}$ (triple heterozygotes, 100%). Among the stage-matched embryos of the three genotypes, similar patterns of expression of *Cer1* in the anterior visceral endoderm, *Foxa2* in the anterior primitive streak (where the progenitor of the organiser derivatives is localised), *Lhx1* in the anterior axial mesendoderm and *Shh* in the anterior notochord underneath the neural plate were

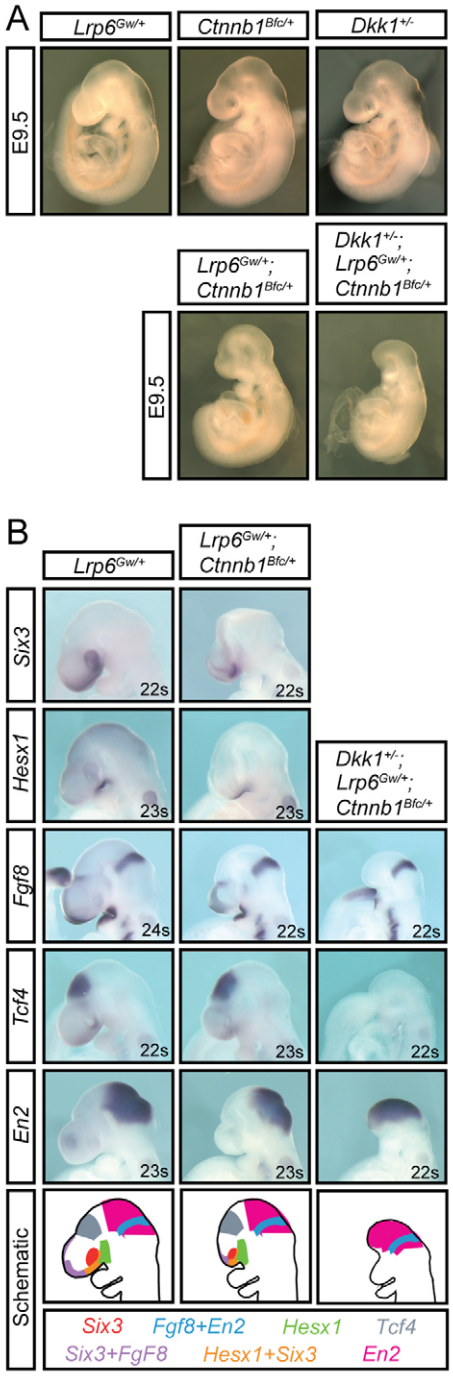

Fig. 7. Phenotype of compound *Lrp6-Gw*, *Ctnnb1-Bfc* and *Dkk1*-null mutant embryos. (**A**) Morphology of E9.5 *Lrp6*$^{Gw/+}$, *Ctnnb1*$^{Bfc/+}$, *Dkk1*$^{+/-}$, *Lrp6*$^{Gw/+}$;*Ctnnb1*$^{Bfc/+}$ and *Dkk1*$^{+/-}$;*Lrp6*$^{Gw/+}$;*Ctnnb1*$^{Bfc/+}$ mutant embryos. (**B**) *Six3*, *Hesx1*, *Fgf8*, *Tcf4* and *En2* expression at E9.5 in *Lrp6*$^{Gw/+}$;*Ctnnb1*$^{Bfc/+}$ and *Dkk1*$^{+/-}$;*Lrp6*$^{Gw/+}$;*Ctnnb1*$^{Bfc/+}$ embryos compared with *Lrp6*$^{Gw/+}$ embryos. The embryos were stage-matched by somite number (s). The gene expression data are collated in a schematic diagram to highlight the differences in the expression domain of the markers (colour-coded) in the forebrain of *Lrp6*$^{Gw/+}$, *Lrp6*$^{Gw/+}$;*Ctnnb1*$^{Bfc/+}$ and *Dkk1*$^{+/-}$;*Lrp6*$^{Gw/+}$;*Ctnnb1*$^{Bfc/+}$ embryos.

observed (see Fig. S4 in the supplementary material). These findings suggest that mutations of these three components of the canonical WNT signalling pathway do not affect the formation or the function of the tissues that are known to influence head formation and that the head truncation observed is primarily caused by changes in the response of the head tissues to elevated WNT signalling activity.

To determine whether the manifestation of the head deficiency/truncation is influenced by allele-specific mutant effects, we analysed the complete set of E9.0-10.0 embryo data by categorising the mutant phenotypes by the degree of severity (Fig. 4B). Analysis of the relative frequency of the different phenotype categories revealed a correlation of the severity of the head phenotype and the genotype: there is increasing disruption of the morphogenesis of the prosencephalon when there are mutations of more than one component of the signalling cascade, and with increasing dosage of mutant alleles individually and in combination (Fig. 8A). It is likely that this phenotypic outcome reflects the degree of gain of canonical WNT function in the different genotype combinations.

To test whether the degree of head truncation is correlated with the gain of WNT signalling function, we measured the level of expression of two known canonical WNT target genes (*Axin2* and *Dkk1*; Fig. 1A) in individual embryos of the five phenotypic categories. To ensure that the embryos were on a comparable strain background, they were generated by crossing *Dkk1*$^{+/-}$;*Lrp6*$^{Gw/Gw}$ male and *Ctnnb1*$^{Bfc/+}$ female mice. The overall distribution of phenotypic categories of embryos derived from this cross was similar to that of the embryos pooled from previous crosses (see Table S7 in the supplementary material). Thirty-four embryos at the 20- to 25-somite stage were selected, categorised and samples of head and body parts were analysed separately by RT-qPCR. Quantification of the level of *Axin2* mRNA in the head samples revealed that expression of this WNT target gene was significantly enhanced with increased degree of head truncation (Fig. 8B). Based on the observation that the response of *Dkk1* to WNT activity is related to the dosage of wild-type allele in the genome (higher in *Dkk1*$^{+/+}$ than *Dkk1*$^{+/-}$ embryos) (Lewis et al., 2008), *Dkk1* expression was analysed separately for mutant embryos of the *Dkk1*$^{+/+}$ and *Dkk1*$^{+/-}$ genotype (Fig. 8B). The findings revealed a significant increase in *Dkk1* expression with the severity of the truncation phenotype for compound mutant embryos with the *Dkk1*$^{+/-}$ genotype. Although not statistically significant, *Dkk1* expression had a tendency to increase in a similar manner in embryos with the *Dkk1*$^{+/+}$ genotype (categories I to III only; Fig. 8B). Despite the elevated activity of *Dkk1* in the compound mutant, the manifestation of the head phenotype indicates that this is not sufficient to antagonise the excess WNT signalling activity. There was no change in the expression of *Sfrp1*, another WNT antagonist, in embryos of the five phenotype categories (see Fig. S5 in the supplementary material), suggesting that there is not any compensatory activity of other antagonists. To rule out a secondary effect on gene expression level due to loss of tissues in the truncated head, we also determined *Axin2* and *Dkk1* expression in the body of the embryo (which showed no evident loss of tissues) to verify the gain of WNT function effect. Similar to the head, the expression of both WNT targets increased in the body samples with the severity of the truncation phenotype (Fig. 8B). These results strongly suggest that the manifestation of the head truncation phenotype is associated with a gain of WNT function due to *Dkk1*-null, *Lrp6-Gw* and *Ctnnb1-Bfc* mutations individually and in combination. Furthermore, the degree of loss of the head or forebrain structures is correlated with the extent of elevation of WNT signalling activity during the formative phase of head morphogenesis (Fig. 8C).

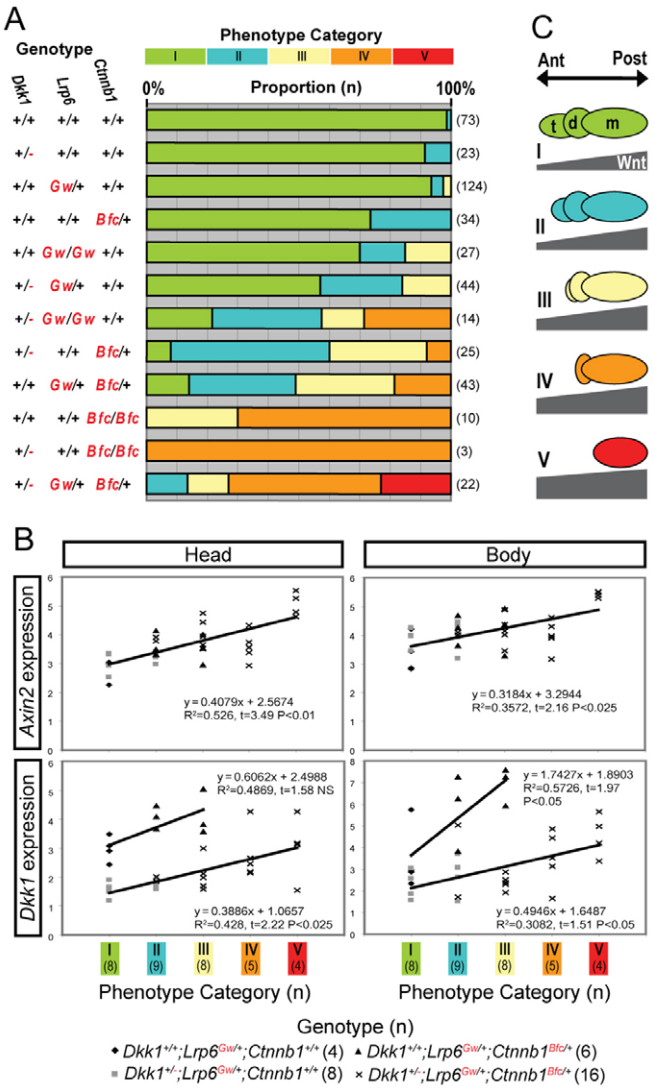

Fig. 8. WNT activity regulates the manifestation of forebrain/head truncation. (**A**) The distribution of embryos of different genotypes to the five head-phenotype categories (I-V). The length of the bar indicates the percentage of embryos in each category (colour-coded). Mutant alleles are highlighted (red text). Number of embryos (n) scored for each genotype is given in parentheses. (**B**) RT-qPCR analysis of the expression of *Axin2* and *Dkk1* relative to β-*actin* expression (Y-axis) in the head and body of mutant embryos showing the positive correlation of the level of gene expression and the severity of the phenotype represented by the five head-phenotype categories (X-axis). Each data point represents the mean value of three independent measures carried out using the cDNA of a single embryo, the genotype of which is identified by a square, a diamond, a triangle or a cross (as indicated). The number of embryos (n) in each phenotype category and for each genotype is indicated in parentheses. The trend line, the equation and the correlation coefficient (R^2) of the linear correlation analysis are indicated in each panel. For the *Dkk1* analysis, the data were analysed separately for embryos of $Dkk1^{+/+}$ genotype (top part of the graph) and $Dkk1^{+/-}$ genotype (bottom part of the graph). The correlation coefficients were tested for significant difference from zero by one-tailed *t*-test (*t* and *P* values indicated; NS, not significant). (**C**) The extent of loss of forebrain structures with reference to the elevation of WNT signalling activity (height of the bar indicates the signal intensity) for each phenotype category. Ant, anterior; Post, posterior; d, diencephalon; m, mesencephalon; t, telencephalon.

DISCUSSION

The findings of this study highlight a functional impact of the level of canonical WNT signalling activity perceived by the progenitor tissues on their differentiation to specific parts of the forebrain and head. The loss of DKK1 has been shown to result in increased WNT signalling activity and causes head truncation (Lewis et al., 2008). In *Xenopus* and zebrafish, DKK1 inhibition of the canonical WNT signalling by sequestration of LRP6 (Mao et al., 2001; Semenov et al., 2001) is required for proper head formation (Caneparo et al., 2007; Kazanskaya et al., 2000; Shinya et al., 2000). In the present study, ENU-mutant mice, harbouring mutations in two components of the canonical WNT signalling cascade – the co-receptor LRP6 and the transcriptional co-activator β-catenin – were used to test for genetic interaction with the *Dkk1* loss-of-function mutant allele. We have shown that in both ENU mutants the expression domain of the Lef-Tcf-*lacZ* reporter expands ectopically to the anterior embryonic tissues that contain the prospective prosencephalon during organogenesis. This ectopic reporter activity can be discerned before the manifestation of the head phenotype, indicating that cells in these tissues are responding inappropriately to LEF-TCF-mediated WNT signalling activity prior to head morphogenesis. Further tests by genetic crosses showed that the tail phenotype of $Lrp6^{Gw/+}$ mice can be decreased or enhanced by reducing the dosage of *Wnt3* or *Dkk1* genes, respectively. For the *Ctnnb1-Bfc* mutant mice, the viability of the $Ctnnb1^{Bfc/+}$ mice was reduced and the incidence of ocular defects was increased when these heterozygotes also carried a *Dkk1*-null allele. Furthermore, expression of a WNT target, *Axin2*, was increased in $Ctnnb1^{Bfc/+}$ and $Ctnnb1^{Bfc/Bfc}$ mutants. Taken together, these findings strongly suggest that the ENU-mutant alleles of *Lrp6* and *Ctnnb1* are causing an increased level of WNT signalling activity, similar to the effect of loss of function of an antagonist such as DKK1.

The impact of the ENU-induced mutation on the function of LRP6 and β-catenin can be deduced from the known function of the specific domains of protein (He et al., 2004; Schneider et al., 2003). Among the *Lrp6* mutations, some are natural point mutations such as the $Lrp6^{Cd}$ allele resulting in gain of WNT function (Carter et al., 2005; Kokubu et al., 2004; Pinson et al., 2000). Like the *Lrp6-Gw* mutation, the *Lrp6-Cd* mutation is localised in the second propeller domain (PD) coding region of the *Lrp6* gene. As LRP6-Cd protein does not show any change in WNT or DKK1 binding activity, the *Lrp6-Gw* mutation might not have any effect on WNT or DKK1 binding either. However, the *Lrp6-Cd* mutation might alter the interaction of LRP6 with MESD (Carter et al., 2005), which acts as a chaperone to compete with both DKK1 and WNT proteins for binding to LRP6 and therefore influences the level of WNT signalling activity (Li et al., 2005). In addition, the mutation might also alter the interaction of LRP6 with R-Spondin via PD2 (Bell et al., 2008) to enhance the WNT signalling activity (Kim et al., 2008).

The $Ctnnb1^{Bfc}$ allele is unique and contrasts with other *Ctnnb1* mutations (Haegel et al., 1995; Huelsken et al., 2000) in its enhancing effect on WNT signalling activity and in that the mutant phenotype encompasses head deficiency and truncation. The *Ctnnb1-Bfc* mutation affects an armadillo repeat that is crucial for the transactivation activity of β-catenin and its interaction with other transcriptional co-regulators (Stadeli et al., 2006; Willert and Jones, 2006), and also affects the interaction with cadherins to mediate cell adhesion (Yap et al., 1997). A previous study has shown that a conditional ablation of β-catenin in the forebrain results in head truncation (Junghans et al., 2005) similar to the

phenotype described in the present study. However, head truncations in this case might be caused by disruption of the interaction of β-catenin with N-cadherin (which affects cell adhesion and the maintenance of epithelial architecture of the neuroepithelium, and triggers cell death leading to the loss of brain structures) as no changes in β-catenin-WNT signalling activity were detected in the prospective telencephalon (Junghans et al., 2005). Our preliminary study indicates that the β-catenin protein with T635K mutation is functional regarding its interaction with N-Cadherin (data not shown). This finding and the upregulation of an endogenous WNT-target (*Axin2*) suggest that in the *Ctnnb1-Bfc* mutant the forebrain truncation phenotype is more likely to be caused by the excessive WNT activity in the telencephalon, a region which would normally not perceive any WNT signal (Fig. 1B).

Although the precise effect of these specific ENU-induced mutations on the function of LRP6 and β-catenin is not fully known, the fact that they both lead to a gain of WNT signalling activity provided a unique opportunity to test the interaction of these signalling pathway components with DKK1. We demonstrated a positive genetic interaction of *Dkk1*, *Lrp6* and *Ctnnb1* highlighting that the antagonist, the co-receptor and the transcriptional co-activator are integrated functionally in the signalling pathway for head formation. In 23% of the triple compound $Dkk1^{+/-};Lpr6^{Gw/+};Ctnnb1^{Bfc/+}$ mutants, the combined effect of the mutant alleles of these three factors is sufficient to account for the phenotypic consequences of the elevated signalling response caused by the complete loss of antagonistic function in the $Dkk1^{-/-}$ mutant. This finding suggests that DKK1 function for head development in mouse might essentially be to repress the canonical WNT pathway, in contrast to zebrafish and *Xenopus* in which DKK1 activity might also influence the WNT-PCP activity (Caneparo et al., 2007).

Our study has also provided insights into the dosage-dependent requirement of canonical WNT signalling activity in head morphogenesis. The different degrees of loss of the forebrain and head structures in the compound mutants of different genotype combinations (ranging from the presence of one mutant allele each of two genes [compound *Dkk1;Lrp6*, *Dkk1;Ctnnb1*, *Lrp6;Ctnnb1* heterozygotes], two mutant alleles of the *Lrp6* or the *Ctnnb1* genes and one mutant allele for *Dkk1* [compound *Lrp6* homozygote with *Dkk1* heterozygote or compound *Ctnnb1* homozygote with *Dkk1* heterozygote] to triple heterozygotes) provides an unique experimental readout of the impact of disrupted WNT signalling activity on forebrain development. Quantitative analysis of the expression of two endogenous WNT targets in these mutants has shown that the outcome of head development is tightly linked to canonical WNT signalling activity, the manifestation of the gradual head truncation phenotype being directly correlated to the progressive increase in the level of canonical WNT signalling activity. Therefore, our results reveal the importance of precise control of the level of canonical WNT signalling activity during normal head formation, which also underlies a differential sensitivity of the rostral tissues of the head and forebrain to the level of WNT signalling activity. The molecular basis of this sensitivity is not known. However, it might be related to the expression of inherently active signal receptors (e.g. those encoded by *Fzd5* and *Fzd8*) and the signal transducers (e.g. LRP5, LRP6 and β-catenin) in the tissues of the anterior region of the embryo (Kemp et al., 2007; Lu et al., 2004; Kelly et al., 2004; Kimura-Yoshida et al., 2005) in which response to WNT proteins (e.g. WNT3) would normally be blocked by the antagonist (e.g. DKK1) (Lewis et al., 2008). Reduction of the antagonist activity or changes in the function of co-receptor and transcription co-activator could raise the signalling activity (Fig. 8) to the threshold level required to elicit WNT downstream activity (Fig. 9), which consequently disrupts morphogenesis during a crucial phase of head formation.

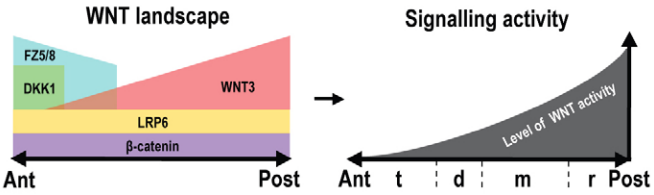

Fig. 9. The WNT landscape and signalling gradient in the head region of early mouse embryo. The left-hand panel depicts the regionalisation of the activity of the ligand (WNT3) (Lewis et al., 2008), the receptor (frizzled 5, frizzled 8; FZ5/8) (Kemp et al., 2007; Lu et al., 2004), the antagonist (DKK1) (Lewis et al., 2008), the co-receptor (LRP6) (Kelly et al., 2004) and the transcriptional co-activator (β-catenin) (Kimura-Yoshida et al., 2005), which translates into a resultant anterior-posterior gradient of signalling activity in the head region of the embryo (depicted in the right-hand panel). Cells in the anterior region of the embryo might be inherently poised to respond to the WNT signal but are suppressed from responding by the activity of the antagonist(s). A low threshold level of signalling activity for eliciting cellular response in the telencephalon and diencephalon might account for the findings that an elevation of the WNT activity leads to preferential loss/reduction of these brain parts. Ant, anterior; Post, posterior; d, diencephalon; m, mesencephalon; r, rhombencephalon; t, telencephalon.

The exceptional sensitivity of the forebrain and associated craniofacial structures to WNT activity highlights the fact that the formation of the embryonic head is contingent on fine-tuned regulation of the domain and level of canonical WNT signalling activity in the progenitor tissues (Lagutin et al., 2003; Lewis et al., 2007; Lewis et al., 2008). In contrast to the impact of loss of WNT antagonist on anterior development, loss of WNT ligand (Yamaguchi et al., 1999) or β-catenin activity, particularly in the posterior embryonic tissues (Yap et al., 1997), leads to failure of the development of posterior structures. It transpires that the anterior-posterior patterning of body parts (in this case, the embryonic head) in the mouse can be mapped onto a WNT landscape where ligands, receptors/co-receptors, trans-activators and antagonists are regionalised and act in concert to establish an ascending gradient of signalling activity in the head-tail dimension (Fig. 9). The organisation of the body plan of the mammalian embryo might, therefore, be accomplished by deploying a WNT-mediated morphogenetic mechanism that is conserved among vertebrate species (Niehrs, 2004; Petersen and Reddien, 2009).

Acknowledgements
Authors thank Thomas Lamonerie for sending reagents, Guillermo Oliver for the *Tcf4* probe, Rebecca Storen for providing mice and David Loebel for critical reading of the manuscript. Animal experimentation has been approved by the CMRI/CHW Animal Care and Ethics Committee. Our work is supported by the NHMRC of Australia (Grant 372103) and Mr James Fairfax. N.F. is a University of Sydney Post-Doctoral Fellow and P.P.L.T. is a NHMRC Senior Principal Research Fellow (Grant 372102).

Competing interests statement
The authors declare no competing financial interests.

Supplementary material
Supplementary material for this article is available at
http://dev.biologists.org/lookup/suppl/doi:10.1242/dev.052803/-/DC1

References

Bell, S. M., Schreiner, C. M., Wert, S. E., Mucenski, M. L., Scott, W. J. and Whitsett, J. A. (2008). R-spondin 2 is required for normal laryngeal-tracheal, lung and limb morphogenesis. *Development* **135**, 1049-1058.

Bogani, D., Warr, N., Elms, P., Davies, J., Tymowska-Lalanne, Z., Goldsworthy, M., Cox, R. D., Keays, D. A., Flint, J., Wilson, V. et al. (2004). New semidominant mutations that affect mouse development. *Genesis* **40**, 109-117.

Brott, B. K. and Sokol, S. Y. (2002). Regulation of Wnt/LRP signaling by distinct domains of Dickkopf proteins. *Mol. Cell. Biol.* **22**, 6100-6110.

Caneparo, L., Huang, Y. L., Staudt, N., Tada, M., Ahrendt, R., Kazanskaya, O., Niehrs, C. and Houart, C. (2007). Dickkopf-1 regulates gastrulation movements by coordinated modulation of Wnt/beta catenin and Wnt/PCP activities, through interaction with the Dally-like homolog Knypek. *Genes Dev.* **21**, 465-480.

Carter, M., Chen, X., Slowinska, B., Minnerath, S., Glickstein, S., Shi, L., Campagne, F., Weinstein, H. and Ross, M. E. (2005). Crooked tail (Cd) model of human folate-responsive neural tube defects is mutated in Wnt coreceptor lipoprotein receptor-related protein 6. *Proc. Natl. Acad. Sci. USA* **102**, 12843-12848.

Fossat, N., Le Greneur, C., Beby, F., Vincent, S., Godement, P., Chatelain, G. and Lamonerie, T. (2007). A new GFP-tagged line reveals unexpected Otx2 protein localization in retinal photoreceptors. *BMC Dev. Biol.* **7**, 122.

Haegel, H., Larue, L., Ohsugi, M., Fedorov, L., Herrenknecht, K. and Kemler, R. (1995). Lack of beta-catenin affects mouse development at gastrulation. *Development* **121**, 3529-3537.

He, X., Semenov, M., Tamai, K. and Zeng, X. (2004). LDL receptor-related proteins 5 and 6 in Wnt/beta-catenin signaling: arrows point the way. *Development* **131**, 1663-1677.

Huelsken, J., Vogel, R., Brinkmann, V., Erdmann, B., Birchmeier, C. and Birchmeier, W. (2000). Requirement for beta-catenin in anterior-posterior axis formation in mice. *J. Cell Biol.* **148**, 567-578.

Inoue, T., Nakamura, S. and Osumi, N. (2000). Fate mapping of the mouse prosencephalic neural plate. *Dev. Biol.* **219**, 373-383.

Junghans, D., Hack, I., Frotscher, M., Taylor, V. and Kemler, R. (2005). Beta-catenin-mediated cell-adhesion is vital for embryonic forebrain development. *Dev. Dyn.* **233**, 528-539.

Kazanskaya, O., Glinka, A. and Niehrs, C. (2000). The role of Xenopus dickkopf1 in prechordal plate specification and neural patterning. *Development* **127**, 4981-4992.

Kelly, O. G., Pinson, K. I. and Skarnes, W. C. (2004). The Wnt co-receptors Lrp5 and Lrp6 are essential for gastrulation in mice. *Development* **131**, 2803-2815.

Kemp, C. R., Willems, E., Wawrzak, D., Hendrickx, M., Agbor Agbor, T. and Leyns, L. (2007). Expression of Frizzled5, Frizzled7, and Frizzled10 during early mouse development and interactions with canonical Wnt signaling. *Dev. Dyn.* **236**, 2011-2019.

Kim, K. A., Wagle, M., Tran, K., Zhan, X., Dixon, M. A., Liu, S., Gros, D., Korver, W., Yonkovich, S., Tomasevic, N. et al. (2008). R-Spondin family members regulate the Wnt pathway by a common mechanism. *Mol. Biol. Cell* **19**, 2588-2596.

Kimura-Yoshida, C., Nakano, H., Okamura, D., Nakao, K., Yonemura, S., Belo, J. A., Aizawa, S., Matsui, Y. and Matsuo, I. (2005). Canonical Wnt signaling and its antagonist regulate anterior-posterior axis polarization by guiding cell migration in mouse visceral endoderm. *Dev. Cell* **9**, 639-650.

Kokubu, C., Heinzmann, U., Kokubu, T., Sakai, N., Kubota, T., Kawai, M., Wahl, M. B., Galceran, J., Grosschedl, R., Ozono, K. et al. (2004). Skeletal defects in ringelschwanz mutant mice reveal that Lrp6 is required for proper somitogenesis and osteogenesis. *Development* **131**, 5469-5480.

Lagutin, O. V., Zhu, C. C., Kobayashi, D., Topczewski, J., Shimamura, K., Puelles, L., Russell, H. R., McKinnon, P. J., Solnica-Krezel, L. and Oliver, G. (2003). Six3 repression of Wnt signaling in the anterior neuroectoderm is essential for vertebrate forebrain development. *Genes Dev.* **17**, 368-379.

Lavado, A., Lagutin, O. V. and Oliver, G. (2008). Six3 inactivation causes progressive caudalization and aberrant patterning of the mammalian diencephalon. *Development* **135**, 441-450.

Lewis, S. L., Khoo, P. L., De Young, R. A., Bildsoe, H., Wakamiya, M., Behringer, R. R., Mukhopadhyay, M., Westphal, H. and Tam, P. P. (2007). Genetic interaction of Gsc and Dkk1 in head morphogenesis of the mouse. *Mech. Dev.* **124**, 157-165.

Lewis, S. L., Khoo, P. L., De Young, R. A., Steiner, K., Wilcock, C., Mukhopadhyay, M., Westphal, H., Jamieson, R. V., Robb, L. and Tam, P. P. (2008). Dkk1 and Wnt3 interact to control head morphogenesis in the mouse. *Development* **135**, 1791-1801.

Li, Y., Chen, J., Lu, W., McCormick, L. M., Wang, J. and Bu, G. (2005). Mesd binds to mature LDL-receptor-related protein-6 and antagonizes ligand binding. *J. Cell Sci.* **118**, 5305-5314.

Liu, P., Wakamiya, M., Shea, M. J., Albrecht, U., Behringer, R. R. and Bradley, A. (1999). Requirement for Wnt3 in vertebrate axis formation. *Nat. Genet.* **22**, 361-365.

Logan, C. Y. and Nusse, R. (2004). The Wnt signaling pathway in development and disease. *Annu. Rev. Cell Dev. Biol.* **20**, 781-810.

Lu, C. C., Robertson, E. J. and Brennan, J. (2004). The mouse frizzled 8 receptor is expressed in anterior organizer tissues. *Gene Expr. Patterns* **4**, 569-572.

MacDonald, B. T., Adamska, M. and Meisler, M. H. (2004). Hypomorphic expression of Dkk1 in the doubleridge mouse: dose dependence and compensatory interactions with Lrp6. *Development* **131**, 2543-2552.

MacDonald, B. T., Tamai, K. and He, X. (2009). Wnt/beta-catenin signaling: components, mechanisms, and diseases. *Dev. Cell* **17**, 9-26.

Mao, B., Wu, W., Li, Y., Hoppe, D., Stannek, P., Glinka, A. and Niehrs, C. (2001). LDL-receptor-related protein 6 is a receptor for Dickkopf proteins. *Nature* **411**, 321-325.

Maretto, S., Cordenonsi, M., Dupont, S., Braghetta, P., Broccoli, V., Hassan, A. B., Volpin, D., Bressan, G. M. and Piccolo, S. (2003). Mapping Wnt/beta-catenin signaling during mouse development and in colorectal tumors. *Proc. Natl. Acad. Sci. USA* **100**, 3299-3304.

Mukhopadhyay, M., Shtrom, S., Rodriguez-Esteban, C., Chen, L., Tsukui, T., Gomer, L., Dorward, D. W., Glinka, A., Grinberg, A., Huang, S. P. et al. (2001). Dickkopf1 is required for embryonic head induction and limb morphogenesis in the mouse. *Dev. Cell* **1**, 423-434.

Niehrs, C. (2004). Regionally specific induction by the Spemann-Mangold organizer. *Nat. Rev. Genet.* **5**, 425-434.

Nolan, P. M., Peters, J., Strivens, M., Rogers, D., Hagan, J., Spurr, N., Gray, I. C., Vizor, L., Brooker, D., Whitehill, E. et al. (2000). A systematic, genome-wide, phenotype-driven mutagenesis programme for gene function studies in the mouse. *Nat. Genet.* **25**, 440-443.

Petersen, C. P. and Reddien, P. W. (2009). Wnt signaling and the polarity of the primary body axis. *Cell* **139**, 1056-1068.

Pinson, K. I., Brennan, J., Monkley, S., Avery, B. J. and Skarnes, W. C. (2000). An LDL-receptor-related protein mediates Wnt signalling in mice. *Nature* **407**, 535-538.

Robb, L. and Tam, P. P. (2004). Gastrula organiser and embryonic patterning in the mouse. *Semin. Cell Dev. Biol.* **15**, 543-554.

Rubenstein, J. L., Shimamura, K., Martinez, S. and Puelles, L. (1998). Regionalization of the prosencephalic neural plate. *Annu. Rev. Neurosci.* **21**, 445-477.

Schneider, S. Q., Finnerty, J. R. and Martindale, M. Q. (2003). Protein evolution: structure-function relationships of the oncogene beta-catenin in the evolution of multicellular animals. *J. Exp. Zool. B Mol. Dev. Evol.* **295**, 25-44.

Semenov, M. V., Tamai, K., Brott, B. K., Kuhl, M., Sokol, S. and He, X. (2001). Head inducer Dickkopf-1 is a ligand for Wnt coreceptor LRP6. *Curr. Biol.* **11**, 951-961.

Shinya, M., Eschbach, C., Clark, M., Lehrach, H. and Furutani-Seiki, M. (2000). Zebrafish Dkk1, induced by the pre-MBT Wnt signaling, is secreted from the prechordal plate and patterns the anterior neural plate. *Mech. Dev.* **98**, 3-17.

Simeone, A., Gulisano, M., Acampora, D., Stornaiuolo, A., Rambaldi, M. and Boncinelli, E. (1992). Two vertebrate homeobox genes related to the Drosophila empty spiracles gene are expressed in the embryonic cerebral cortex. *EMBO J.* **11**, 2541-2550.

Stadeli, R., Hoffmans, R. and Basler, K. (2006). Transcription under the control of nuclear Arm/beta-catenin. *Curr. Biol.* **16**, R378-R385.

Tam, P. P. (1989). Regionalisation of the mouse embryonic ectoderm: allocation of prospective ectodermal tissues during gastrulation. *Development* **107**, 55-67.

Willert, K. and Jones, K. A. (2006). Wnt signaling: is the party in the nucleus? *Genes Dev.* **20**, 1394-1404.

Yamaguchi, T. P., Bradley, A., McMahon, A. P. and Jones, S. (1999). A Wnt5a pathway underlies outgrowth of multiple structures in the vertebrate embryo. *Development* **126**, 1211-1223.

Yao, J. and Kessler, D. S. (2001). Goosecoid promotes head organizer activity by direct repression of Xwnt8 in Spemann's organizer. *Development* **128**, 2975-2987.

Yap, A. S., Brieher, W. M. and Gumbiner, B. M. (1997). Molecular and functional analysis of cadherin-based adherens junctions. *Annu. Rev. Cell Dev. Biol.* **13**, 119-146.

Table S1. Genotype distribution and frequency of tail defects in *Lrp6-Gw* mutant mice

A: Mice from *Lrp6*$^{Gw/+}$ × *Lrp6*$^{Gw/+}$ intercrosses

	Distribution of genotypes: number (%)†	Number displaying tail kink phenotype/number analyzed (%):
Wild type	43 (27)	0/24 (0)
Lrp6$^{Gw/+}$	83 (52)	25/37 (67.5)*
Lrp6$^{Gw/Gw}$	34 (21)	6/7 (85.5)*

B. Mice from *Dkk1*$^{+/-}$ × *Lrp6*$^{Gw/+}$ and *Wnt3*$^{+/-}$ × *Lrp6*$^{Gw/+}$ intercrosses

	Number displaying tail kink phenotype/number analyzed (%):
Wild type	0/27 (0)
Wnt3$^{+/-}$	0/13 (0)
Dkk1$^{+/-}$	0/16 (0)
Lrp6$^{Gw/+}$	18/26 (69)
Wnt3$^{+/-}$;*Lrp6*$^{Gw/+}$	3/14 (21.5)**
Dkk1$^{+/-}$;*Lrp6*$^{Gw/+}$	16/16 (100)**

Strain background: *Lrp6-Gw* mice, C3H/HeH; *Dkk1* mutant mice, C57BL/6; *Wnt3* mutant mice, C57BL/6.
†Not different from the expected Mendelian distribution.
Significantly different from wild type at *P<0.001, and from *Lrp6*$^{Gw/+}$ at **P<0.005 by χ^2-test.

Table S2. Genotype distribution and incidence of head malformations in E10.0-11.0 *Lrp6-Gw* mutant embryos[†]

Genotype	Distribution of genotypes: number (%)*	Number of embryos with head defects/number analyzed (%)
Wild type	15 (23)	0/15 (0)
Lrp6$^{Gw/+}$	37 (57)	2/37 (5.5)
Lrp6$^{Gw/Gw}$	13 (20)	5/13 (38.5)**

[†]*Lrp6*$^{Gw/+}$ × *Lrp6*$^{Gw/+}$ intercrosses, C3H/HeH background.
*Not different from the expected Mendelian distribution.
**Significantly different from wild type at $P<0.01$ by χ^2-test.

Table S3. Frequency of head malformations in *Lrp6-Gw* and *Ctnnb1-Bfc* mutant embryos on a *Dkk1*$^{+/-}$ background

A. Compound *Dkk1*-null;*Lrp6-Gw* mutant embryos†

	Number of embryos showing head defects/number analyzed (%)		
Genotype	E9.0-10.0	E10.0-11.0	Overall
Wild type	0/0	0/5 (0)	0/5 (0)
Dkk1$^{+/-}$	0/0	0/6 (0)	0/6 (0)
Lrp6$^{Gw/+}$	2/30 (6.5)	2/12 (16.5)	4/42 (9.5)
Dkk1$^{+/-}$;*Lpr6*$^{Gw/+}$	10/22 (45.5)	1/6 (16.5)	11/28 (39.5)
Lrp6$^{Gw/Gw}$	3/9 (33)	0/0	3/9 (33)
Dkk1$^{+/-}$;*Lpr6*$^{Gw/Gw}$	9/10 (90)	2/4 (50)	11/14 (78.5)*

B. Compound *Dkk1*-null;*Ctnnb1-Bfc* mutant embryos‡

	Number of embryos showing head defects/number analyzed (%)			
Genotype	E8.0-9.0	E9.0-10.0	E10.0-11.0	Overall
Wild type	0/0	1/23 (4.5)	0/0	1/23 (4.5)
Dkk1$^{+/-}$	0/0	2/21 (9.5)	0/1 (0)	2/22 (9)
Ctnnb1$^{Bfc/+}$	0/2 (0)	5/14 (35)	0/6 (0)	5/22 (23)
Dkk1$^{+/-}$;*Ctnnb1*$^{Bfc/+}$	0/0	20/21 (95)	0/0	20/21 (95)**
Ctnnb1$^{Bfc/Bfc}$	0/0	2/2 (100)	0/0	2/2 (100)§
Dkk1$^{+/-}$;*Ctnnb1*$^{Bfc/Bfc}$	4/4 (100)	3/3 (100)	0/0	7/7 (100)**

Background: *Lrp6-Gw* mice, C3H/HeH; *Ctnnb1-Bfc* mice, BALB/c; *Dkk1* mutant mice, C57BL/6.

†From three intercrosses: *Dkk1*$^{+/-}$ × *Lrp6*$^{Gw/+}$, *Dkk1*$^{+/-}$ × *Lrp6*$^{Gw/Gw}$ and *Dkk1*$^{+/-}$;*Lpr6*$^{Gw/+}$ × *Lrp6*$^{Gw/Gw}$.

‡From two intercrosses: *Dkk1*$^{+/-}$ × *Ctnnb1*$^{Bfc/+}$ and *Dkk1*$^{+/-}$;*Ctnnb1*$^{Bfc/+}$ × *Ctnnb1*$^{Bfc/+}$.

Significantly different from wild type at *P<0.005 and **P<0.001 by χ^2-test.

§Sample size too small for testing.

Table S4. Genotype distribution and frequency of morphological defects in *Ctnnb1-Bfc* mutant mice

A. Mice from *Ctnnb1*$^{+/+}$ × *Ctnnb1*$^{Bfc/+}$ intercrosses on two backgrounds

Genotype (background)	Distribution of genotypes: number (%)	Number of mice showing Bat-like face/number analyzed (%)	Number of mice showing ocular defects/number analyzed (%)
Wild type (C57BL/6)	160 (73)†	0/30 (0)	0/30 (0)
Ctnnb1$^{Bfc/+}$ (C57BL/6)	59 (27)†	13/13 (100)**	3/13 (23)*
Wild type (BALB/c)	96 (61.5)†	0/26 (0)	0/26 (0)
Ctnnb1$^{Bfc/+}$ (BALB/c)	60 (38.5)†	19/19 (100)**	2/19 (10.5)

B. Mice from *Dkk1*$^{+/-}$ × *Ctnnb1*$^{Bfc/+}$ intercrosses[§]

Genotype	Distribution of genotypes: number (%)‡	Number of mice showing ocular defects/number analyzed (%)
Wild type	75 (37)	0/10 (0)
Dkk1$^{+/-}$	64 (31.5)	0/13 (0)
Ctnnb1$^{Bfc/+}$	53 (26)	0/8 (0)
Dkk1$^{+/-}$;*Ctnnb1*$^{Bfc/+}$	11 (5.5)	5/7 (71.5)**

Significantly different from expected Mendelian distribution at $^{\dagger}P<0.01$ and $^{\ddagger}P<0.001$ by χ^2-test.
Significantly different from wild type at $*P<0.01$ and $**P<0.001$ by χ^2-test.
[§]Background: *Dkk1* mutant mice, C57BL/6; *Ctnnb1-Bfc* mice, BALB/c.

Table S5. Genotype distribution and incidence of head malformations in *Ctnnb1-Bfc* mutant embryos†

	Distribution of genotypes: number (%)*					Number of mice with head defects/number analyzed (%)			
Genotype	E7.0-8.0	E8.0-9.0	E9.0-10.0	E10.0-11.0	Overall	E7.0-8.0	E8.0-9.0	E9.0-10.0	E10.0-11.0
Wild type	3 (21)	1 (11)	8 (26.5)	3 (37.5)	15 (24.5)	0/3 (0)	0/1 (0)	0/8 (0)	0/3 (0)
Ctnnb1$^{Bfc/+}$	7 (50)	8 (89)	15 (50)	4 (50)	34 (56)	0/7 (0)	3/8 (37.5)‡	14/15 (93.5)**	3/4 (75)
Ctnnb1$^{Bfc/Bfc}$	4 (28.5)	0 (0)	7 (23.5)	1 (12.5)	12 (19.5)	0/4 (0)	0/0	7/7 (100)**	1/1 (100)‡

†From *Ctnnb1*$^{Bfc/+}$ × *Ctnnb1*$^{Bfc/+}$ intercrosses, C57BL/6 background.
*Not different from the expected Mendelian distribution.
**Significantly different from wild type at $P<0.001$ by χ^2-test.
‡Sample size too small for testing.

Table S6. Frequency of head malformations in compound *Dkk1*-null;*Lrp6-Gw;Ctnnb1-Bfc* mutant embryos at E9.0-10.0†

Genotype	Number of embryos showing head defects/number analyzed (%)
Wild type	0/15 (0)
Dkk1$^{+/-}$	0/2 (0)
Lrp6$^{Gw/+}$	2/42 (5)
Ctnnb1$^{Bfc/+}$	3/20 (15)
Dkk1$^{+/-}$;*Lpr6*$^{Gw/+}$	8/16 (50)*
Dkk1$^{+/-}$;*Ctnnb1*$^{Bfc/+}$	3/4 (75)*
Lpr6$^{Gw/+}$;*Ctnnb1*$^{Bfc/+}$	37/43 (86)*
Dkk1$^{+/-}$;*Lpr6*$^{Gw/+}$;*Ctnnb1*$^{Bfc/+}$	22/22 (100)*

Background: *Lrp6-Gw* mice, C3H/HeH; *Ctnnb1-Bfc* mice, BALB/c; *Dkk1* mutant mice, C57BL/6.

†From four intercrosses: *Lpr6*$^{Gw/+}$ × *Ctnnb1*$^{Bfc/+}$, *Lpr6*$^{Gw/Gw}$ × *Ctnnb1*$^{Bfc/+}$, *Dkk1*$^{+/-}$;*Lpr6*$^{Gw/+}$ × *Ctnnb1*$^{Bfc/+}$ and *Dkk1*$^{+/-}$;*Lpr6*$^{Gw/Gw}$ × *Ctnnb1*$^{Bfc/+}$.

*Significantly different from wild type at $P<0.001$ by χ^2-test.

Table S7. Distribution of phenotype category of mutant embryos with head defects

Genotype	Number of embryos	% with head defects	Head phenotype category			
			II	III	IV	V
Pooled samples (data extracted from Table 1 and Figure 6)						
Dkk1$^{+/+}$;*Lrp6*$^{Gw/+}$; *Ctnnb1*$^{+/+}$	124	6.5	6	2		
Dkk1$^{+/+}$;*Lrp6*$^{Gw/+}$;*Ctnnb1*$^{Bfc/+}$	43	86	15	15	7	
Dkk1$^{+/-}$; *Lrp6*$^{Gw/+}$;*Ctnnb1*$^{+/+}$	44	43.2	11	8		
Dkk1$^{+/-}$;*Lrp6*$^{Gw/+}$;*Ctnnb1*$^{Bfc/+}$	22	100	3	2	12	5
	233*		35 (40.7%)	27 (31.4%)	19 (22.1%)	5 (5.8%)
Specific cross: *Ctnnb1*$^{Bfc/+}$ × *Dkk1*$^{+/-}$;*Lrp6*$^{Gw/Gw}$						
Dkk1$^{+/+}$;*Lrp6*$^{Gw/+}$; *Ctnnb1*$^{+/+}$	4	0				
Dkk1$^{+/+}$;*Lrp6*$^{Gw/+}$;*Ctnnb1*$^{Bfc/+}$	6	100	3	3		
Dkk1$^{+/-}$; *Lrp6*$^{Gw/+}$;*Ctnnb1*$^{+/+}$	8	50	4			
Dkk1$^{+/-}$;*Lrp6*$^{Gw/+}$;*Ctnnb1*$^{Bfc/+}$	16	100	2	5	5	4
	34*		9 (34.6%)	8(30.7%)	5 (19.2%)	4 (15.3%)

*No significant difference in the distribution of phenotype categories II-IV between embryos of the pooled sample and the specific cross by Chi-squared test: χ^2=2.527, P>0.05